Chapter 4

C/Li_2MnSiO_4 Nanocomposite Cathode Material for Li-Ion Batteries

Marcin Molenda, Michał Świętosławski and Roman Dziembaj

Additional information is available at the end of the chapter

http://dx.doi.org/10.5772/48319

1. Introduction

Technological development of portable devices, e.g, mobile phones, laptops, etc., as well as progress in electrical vehicles (EV) and hybrid electrical vehicles (HEV) technologies require batteries efficient in volumetric and gravimetric energy storage, exhibiting large number of charge/discharge cycles and being cheap and safe for users. Moreover, materials used in energy storage and conversion systems should be environmentally friendly and recyclable. Currently, rechargeable lithium-ion batteries (LIBs) are the most popular portable energy storage system, mostly due to their highest energy density among all others rechargeable battery technologies, like Ni-Cd or Ni-MH cells which reached the theoretical limit of performance. Commercially available LIBs are based on layered lithium cobalt oxide ($LiCoO_2$) or related systems, which are expensive and toxic. These materials are unstable in an overcharged state, thus the battery safety is affected, especially in high power (20-100 kWh) applications for EV, HEV and renewable energy systems. The bigger battery capacity results in more energy accumulated, thus operational safety is a key issue. On the other hand, lifetime and capacity retention of LIBs in changeable operation conditions (from -30°C to +60°C, average lifetime 2-4 years) are a challenges to develop new materials and cell assembly technologies.

2. Li-ion battery technology

First rechargeable lithium cells taking advantages of intercalation process were developed in year 1972 [1]. The cells $Li/Li^+/Li_xTiS_2$ revealed 2V potential and relatively low gravimetric capacity. Applications of metallic lithium as anode material resulted in common cell breakdown due to formation of dendritic structures on anode during cell cycling. The problems forced research and development of new intercalation materials for lithium batteries. In the eighties a new conception of lithium cell was proposed (so called Li-ion

batteries or "rocking-chair batteries"), which consisted of application of two different lithium intercalation compounds as anode and cathode materials [2-4]. As anode material a graphite intercalated with lithium was used while cathode materials were based on layered 3d transition metal oxides.

2.1. Layered $LiCoO_2$ oxide and related systems

The first $Li_xC_6/Li^+/Li_{1-x}CoO_2$ Li-ion battery system was commercialized in 1993 by Sony Co. In Fig. 1 a working mechanism during discharge cycle of Li-ion cell is presented.

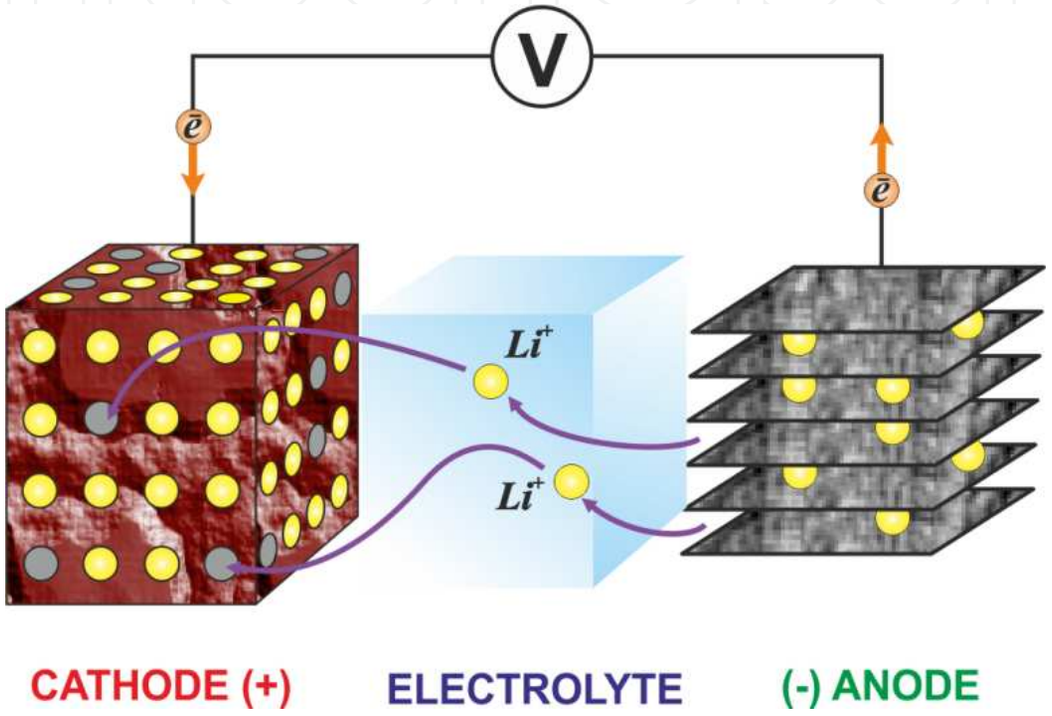

Figure 1. Working mechanism of Li-ion batteries (discharge cycle).

The electrochemical reaction at the graphite anode side can be written as (1):

$$C_6 + xLi^+ + xe^- \leftrightarrow Li_xC_6 \quad (1)$$

and suitably at $LiCoO_2$ cathode side (2):

$$LiCoO_2 \leftrightarrow Li_{1-x}CoO_2 + xLi^+ + xe^- \quad (2)$$

Commercially available LIBs based on layered lithium cobalt oxide ($LiCoO_2$) or related systems ($LiNi_yCo_{1-y}O_2$, $LiMn_yCo_{1-y}O_2$, $LiMn_{1/3}Ni_{1/3}Co_{1/3}O_2$) reveal reversible capacity 130-150 mAh/g and working potential 3.6-3.7 V. The oxide materials are expensive and toxic due to cobalt content and are unstable in an overcharged state, thus the safety is strongly affected. This is related to strong oxidizing behavior of the charged layered oxide cathode in contact with organic electrolyte what may lead to combustion or even explosion [4, 5]. Unfortunately, this effect may be also increased by application of nanosized materials with high surface area.

2.2. Spinel $LiMn_2O_4$ and related systems

An alternative material for cathode based on layered oxides $LiM_yCo_{1-y}O_2$ (M=Ni, Mn, Fe) is $LiMn_2O_4$ spinel. $LiMn_2O_4$ reveals a little lower reversible capacity 120 mAh/g at working potential 4 V, but the material is distinctly cheaper and nontoxic. However, application of spinel as cathode material in commercial Li-ion batteries is retarded by phase transition observed near room temperature, i.e. battery operation temperature, and related to Jahn-Teller distortion of Mn^{3+} ions, what resulted in capacity fading. Stabilization of cubic spinel structure is possible by controlled formation of cationic defects [6], by lithium [7] or 3d metal substitution [8] into spinel lattice as well as by isoelectronic sulfur substitution [9, 10]. Instability of high oxidation state of transition metal in spinel structure observed in charged state of cathode leads to oxygen evolution, similarly to the layered oxide cathodes, and reaction with electrolyte. Application of spinel based materials is limited to cheap battery packs for EV [11].

2.3. Olivine $LiFePO_4$ cathode material

An interesting and very promising group of insertion materials are $LiMXO_4$ (M= metal 3d, X=S, P, As, Mo, W) type compounds [12], with $LiFePO_4$ among them. $LiFePO_4$ lithium iron phosphate of olivine structure is chemically and thermally stable material with relatively high gravimetric capacity 170 mAh/g at working potential 3.5 V. The material is cheap, nontoxic and environmental friendly. Its high chemical stability towards electrolyte, related to strong P-O bonds, significantly improves safety of LIBs. However, very low electrical conductivity of $LiFePO_4$ system (10^{-9} S/cm @RT) requires application of carbon coatings and composite formation [13, 14].

3. Orthosilicates Li_2MSiO_4 – New high capacity cathode materials

Application of orthosilicates Li_2MSiO_4 (M=Fe, Mn, Co, Ni) compounds as insertion materials for LIBs was firstly proposed by Prof. Goodenough [12, 15]. The materials mainly crystallizes in orthorhombic system of Pmn21 space group in olivine structure [16-18]. The Li_2MSiO_4 olivine structure may be described as wavy layers of $[SiMO_4]_\infty$ on *ac* axis plane and connected along *b* axis by LiO_4 tetrahedra [16]. Within the layers every tetrahedron SiO_4 shares its corner with four next MO_4 tetrahedra. Lithium ions occupy the tetrahedral sites (LiO_4) between two layers and share 3 and 1 oxygen atoms with the layers. In fact, diffusion of lithium ions in this structure is possible only through the canals formed by LiO_4 tetrahedra. Li_2MSiO_4 silicates reveal a possibility of reversible insertion of two lithium ions per molecule, so this leads to exchange of two electrons by transition metal. As a results the silicates reveal very high theoretical gravimetric capacity, up to 330 mA/g. However, structural limitation due to sharing of LiO_4 between two wavy layers, should affect a little the capacity. Calculations of electrochemical potential of lithium insertion/deinsertion show a two stage process:

$$Li_2M^{2+}SiO_4 \rightarrow \square LiM^{3+}SiO_4 + Li^+ \quad (3)$$

$$\Upsilon LiM^{3+}SiO_4 \rightarrow \Upsilon_2 M^{4+}SiO_4 + Li^+ \quad (4)$$

Depending on transition metal potential of the reaction (3) vary from 3.2 V (for Fe) to 4.1-4.4 V (for Mn, Co, Ni), while the potential of reaction (4) is in range 4.5-5.0 V. Deinsertion of the second lithium ion requires applying high potential above 4.5 V, and this is a challenge for electrolyte. Orthosilicates Li_2MSiO_4 (M=Fe, Mn, Co, Ni) materials reveal very low electrical conductivity (10^{-12} - 10^{-15} S/cm @RT) and carbon coating of the materials is required. On the other hand, downsizing of material grains should improve electrochemical performance [18]. Very strong covalent bonding of Si-O results in high chemical stability towards electrolyte, strongly increasing the safety of LIBs based on silicates. The materials are nontoxic, environmental friendly and cheap. The properties mentioned above provide a challenge for developing a composite cathode materials based on Li_2MSiO_4 orthosilicates.

4. Li_2MnSiO_4 nanostructured cathode material

Li_2MnSiO_4 is a member of dilithiumorthosilicates Li_2MSiO_4 (M = Fe, Mn, Co) family, thanks to strong covalent Si-O bond, it shows high thermal and chemical stability. High theoretical capacity 333 mAh/g, low production costs, safety and optimal working potential make them an attractive cathode material. Very low electrical conductivity (10^{-12} - 10^{-15} S/cm @RT) can be improved by coating with conductive carbon layers (CCL) and by grains size downsizing [18-20]. The properties of Li_2MnSiO_4 material comes to a conclusion that cathode material for LIBs based on this compound should be prepared as C/Li_2MnSiO_4 nanocomposite. Thus, the special preparation techniques have to be applied in terms to obtain nanocrystaline grains of Li_2MnSiO_4 cathode material coated by conductive carbon layers (CCL). During last few years several different technics of Li_2MnSiO_4 synthesis were proposed. Hydrothermal synthesis [21-24] as well as solid-state reactions [25-28] can lead to one phase product but the control of the grain size is significantly limited. Sol-gel method is one of the soft chemistry techniques which can be used in synthesis of nanosized lithium orthosilicates [29-33]. Sol-gel processes, especially Pechini's method is a simple technic, characterized by low cost and low temperature of treatment, resulting in homogenous, high purity materials.

4.1. Preparation of nanostructured Li_2MnSiO_4

Li_2MnSiO_4 was produced using sol-gel synthesis – Pechini type. Starting reagents were: lithium acetate dihydrate (Aldrich), manganese acetate tetrahydrate (Aldrich), tetraethoxysilane (TEOS) (98%, Aldrich) as a source of silicon, ethylene glycol (POCh), citric acid (POCh) and ethanol (POCh). Thanks to chelating metal ions in solution by citric acid the cations can be mixed at the molecular level and the stoichiometric composition can be achived. The reactants were mixed in a molar ratio 1:1:18:6:4:16 - $Mn:Si:C_2H_6O_2:C_6H_8O_7:C_2H_5OH:H_2O$. Based on previous studies it was affirmed, that using 20% excess of lithium acetate leads to one-phase product. All reagents were dissolved in glass reactor under constant argon flow (Ar 5.7). As a solvent, only stoichiometric amount of distilled water was used. Heating water to 35 °C assure fast and complete dissolution of

metal acetates. Prepared mixture was heated to 60 ˚C and few drops of concentrated hydrochloric acid was added to initiate polymerization of metal citrates using ethylene glycol and TEOS. Reaction was conducted for 24h in close reactor. Obtained gel was aged for 3 days at 60 ˚C in close reactor (Ar atmosphere) and for 3 days at 60 ˚C in an air-drier (Air atmosphere).

Thermogravimetric analysis (TGA) coupled with simultaneous differential thermal analysis (SDTA) and mass spectrometry evolved gas analysis (MS-EGA) of precursor were performed in Mettler-Toledo 851ᵉ thermo-analyzer using 150 µl corundum crucibles under flow of air/argon (80 ml/min), within temperature range 20–800 °C with heating rate of 10 °C/min. The simultaneous MS-EGA was performed in on-line joined quadruple mass spectrometer (QMS) (Thermostar-Balzers). The 17, 18 and 44 m/z mass lines, ascribed to OH, H_2O and CO_2 species respectively, were collected during the TGA experiments. TGA of the Li_2MnSiO_4 precursor are shown in the Fig. 2 and Fig. 3.

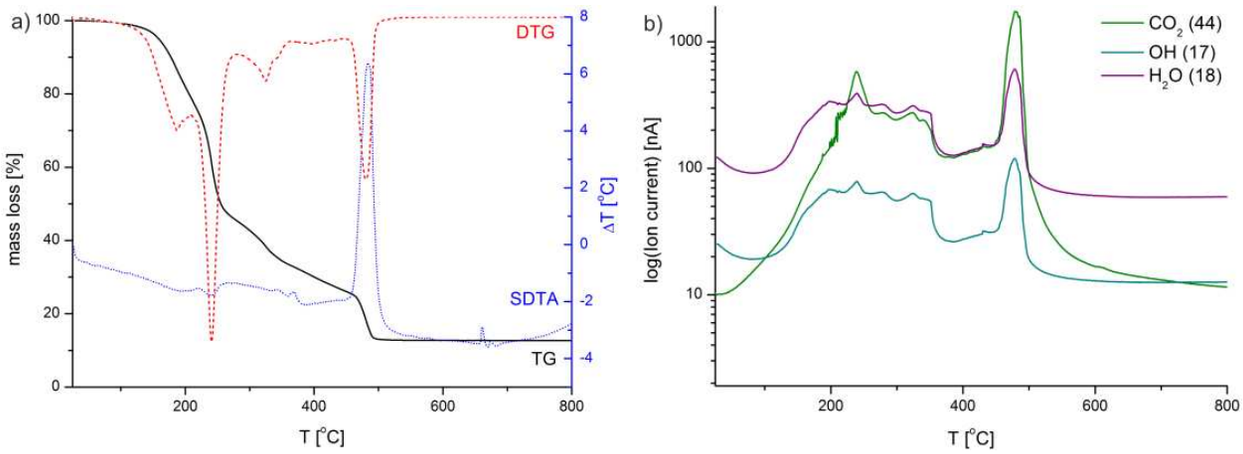

Figure 2. Thermal analysis (TGA/DTG/SDTA) conducted under air atmosphere (a) with evolved gas analysis (EGA-QMS) (b) of Li_2MnSiO_4 precursor.

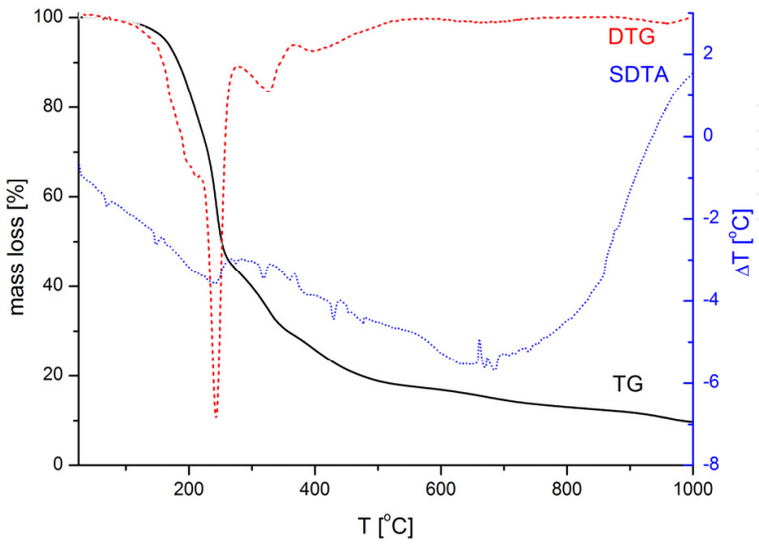

Figure 3. Thermal analysis (TGA/DTG/SDTA) of Li_2MnSiO_4 precursor performed under inert atmosphere (Ar 5.0).

According to TGA curve (Fig. 2a) a complete decomposition of gel organic matrix occurs above 500 °C. Evolved gas analysis confirmed the disintegration of organic components. Amount of active material can be estimated at about 12 wt.% of the precursor. Basing on TGA results calcination conditions were chosen. Li_2MnSiO_4 precursor was calcined under Ar flow at 600, 700, 800 and 900 °C.

4.2. Properties of nanostructured Li_2MnSiO_4

X-ray powder diffraction patterns of the samples were collected on BRUKER D2 PHASER using Cu K_α radiation = 1.5418 Å. In Fig. 4 XRD patterns of Li_2MnSiO_4 obtained at different temperatures (600, 700, 800 and 900 °C) are collected.

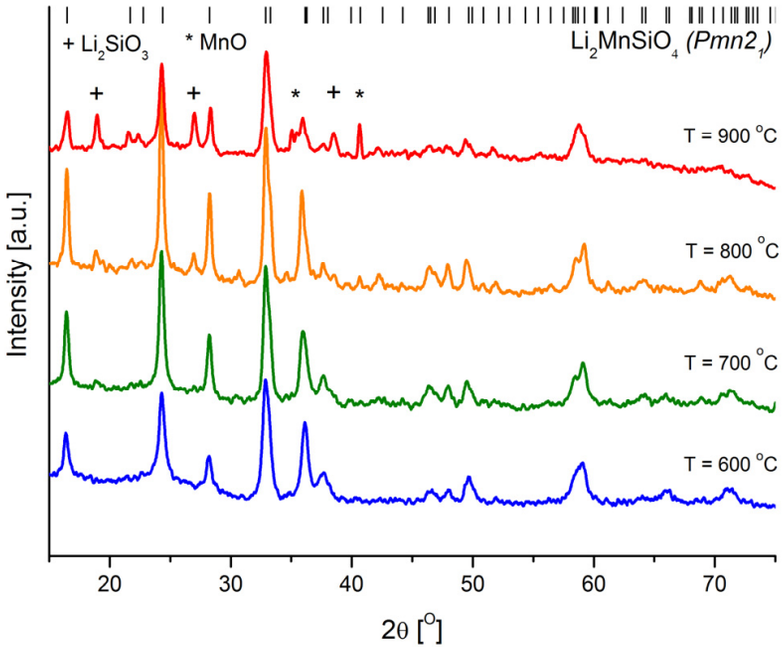

Figure 4. XRD patterns of Li_2MnSiO_4 after calcination at 600 °C, 700 °C, 800 °C and 900 °C. Li_2MnSiO_4 (*Pmn2₁* phase) diffraction lines positions are marked in the top of the figure.

In the sample calcined at 600 °C all diffraction lines can be attributed to pure Li_2MnSiO_4 phase (*Pmn2₁*). In other specimens obtained at higher temperatures, MnO and Li_2SiO_3 impurities starts to appear. Formation of MnO and Li_2SiO_3 in samples calcined at temperatures above 700 °C can be connected, with Li_2MnSiO_4 decomposition. Average crystallites sizes calculated from diffraction lines broadening based on Scherrer equation are in the range of 17-19 nm depending on calcination temperature of the sample (Tab. 1). The calcination under carefully selected conditions leads to a transformation of a part of organic compounds from the gel matrix into thick carbon layer covering the active material. The temperature programmed oxidation (TPO) performed using TGA equipment confirmed presence of carbon in samples. Fig. 5b presents exemplary TG/DTG/SDTA curves from TPO conducted under air flow in temperature range of 20-1000 °C. The amounts of carbon in samples calcined in different temperatures were calculated from TPO measurements and are collected in Table 1.

Measurements of the specific surface area of the samples were performed in Micrometrics ASAP 2010 using BET isotherm method. About 500 mg of each sample was preliminary degassed at 250–300 °C for 3 h under pressure 0.26–0.4 Pa. Then, N_2 sorption was performed at pressure of $8 \cdot 10^4$ Pa. One of pore size distribution plot with the adsorption-desorption curves inset is presented in Fig. 5a. Exact values of specific surface area and average pores diameters are presented in table 1.

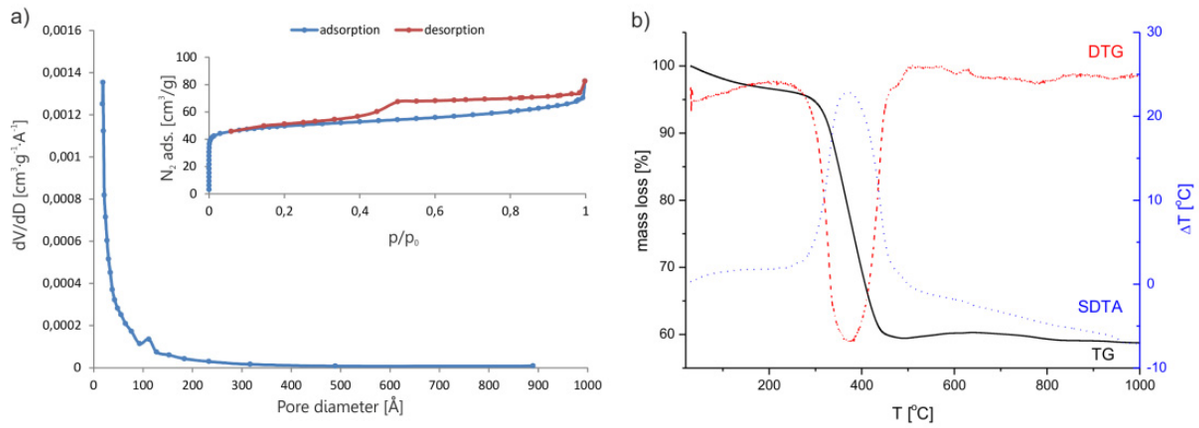

Figure 5. Adsorption-desorption isotherm and pore diameter distribution of C/Li_2MnSiO_4 calcined at 600°C, b) TGA/DTG/SDTA curves of C/Li_2MnSiO_4 calcined at 600 °C.

Low temperature N_2-adsorption (BET) measurements of C/Li_2MnSiO_4 composites show that specific surface area of samples decrease with increasing calcination temperature. Decrease of specific surface area is connected with graphitization of carbon during calcination at higher temperatures.

Sample name	Precursor calcination temperature	Carbon content	Specific surface area (BET)	Average pore dimension (BJH)	Crystallite size (from XRD)
C/Li_2MnSiO_4@600	600 °C	34%	169 m^2/g	50 Å	17 nm
C/Li_2MnSiO_4@700	700 °C	32%	152 m^2/g	72 Å	18 nm
C/Li_2MnSiO_4@800	800 °C	32%	144 m^2/g	73 Å	19 nm
C/Li_2MnSiO_4@900	900 °C	35%	57 m^2/g	73 Å	19 nm

Table 1. Morphology parameters of C/Li_2MnSiO_4 composites calcined at different temperatures.

Electrical conductivity was measured using the AC (33Hz) 4-probe method within temperature range of -40÷55 °C. The carbon coated composite powders were so elastic that the standard preparation of pellets was impossible. The fine powder samples were placed into a glass tube and pressed by a screw-press between parallel gold disc electrodes (Ø=5 mm) till the measured resistance remained constant. The results of electrical conductivity measurements are gather in Fig. 6. All composites exhibit good electrical conductivity (up to 0,36 S/cm for C/Li_2MnSiO_4@900) in comparison with Li_2MnSiO_4 itself (~ 10^{-15} S/cm at room

temperature - RT). It can be observed that temperature dependence of conductivity for composites calcined at higher temperatures (700, 800 and 900 °C) seem unaffected, by temperature (metallic-like behavior). Conductivity value and its invariability against temperature indicate that carbon layers consist of graphite-like domains. In case of C/Li_2MnSiO_4@600°C the carbon layers is more disordered and probably consist of an activated-like carbon. Those results are consistent with BET measurements in case of graphitization process occurring at higher temperatures.

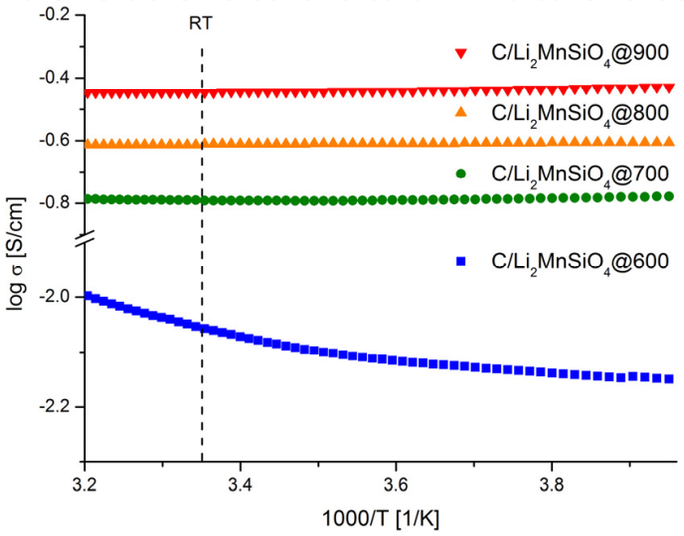

Figure 6. Electrical conductivity measurement of C/Li_2MnSiO_4 (temp. range: -20 to 40°C). Dash line represent room temperature (RT).

Selected samples were investigated using transmission electron microscope (TEM) (Fig. 7 and Fig. 8). Micrographs were collected on TECNAI G2 F20 (200 kV) coupled with an energy dispersive X-ray spectrometer (EDAX).

TEM micrographs reveal well dispersed lithium manganese orthosilicate grains (dark grey and black dots) in the carbon matrix. Figures 7a; 7c; 7d present C/Li_2MnSiO_4@600 at different magnifications. Fig. 7b shows STEM-HAADF (*Scanning Transmission Electron Microscopy – High Angular Annular Dark Field*) image of the C/Li_2MnSiO_4@600 composite. Energy dispersive X-ray spectroscopy (EDS) (Fig. 7b1; 7b2) confirmed presence of lithium manganese silicate in the spots marked in the micrograph 7b (Cu peaks in all EDS spectra originate from TEM copper grid). High resolution electron microscopy image (HREM) shows single grain of Li_2MnSiO_4 (Fig. 7e). Corresponding to that IFFT (*Inverse Fast Furrier Transform*) image (Fig. 7f) clearly shows a crystalline structure of obtained material which can be identified as Li_2MnSiO_4. Grains in the composite have sizes in a range of 5-10 nm. Microstructure of a C/Li_2MnSiO_4 composite calcined at 700 °C is shown in Fig. 8. C/Li_2MnSiO_4@700 °C composite has a bimodal distribution of a crystallite size. TEM micrographs show presence of small (5-10 nm) Li_2MnSiO_4 crystallites, analogues of C/Li_2MnSiO_4@600 °C and a bigger, well crystallized silicates grains, in a range of 50-150 nm (Fig. 8a, c, d). Both types of crystallites in the sample have the same composition which is confirmed by EDS analysis presented in fig. 8b_1, b_2, b_3.

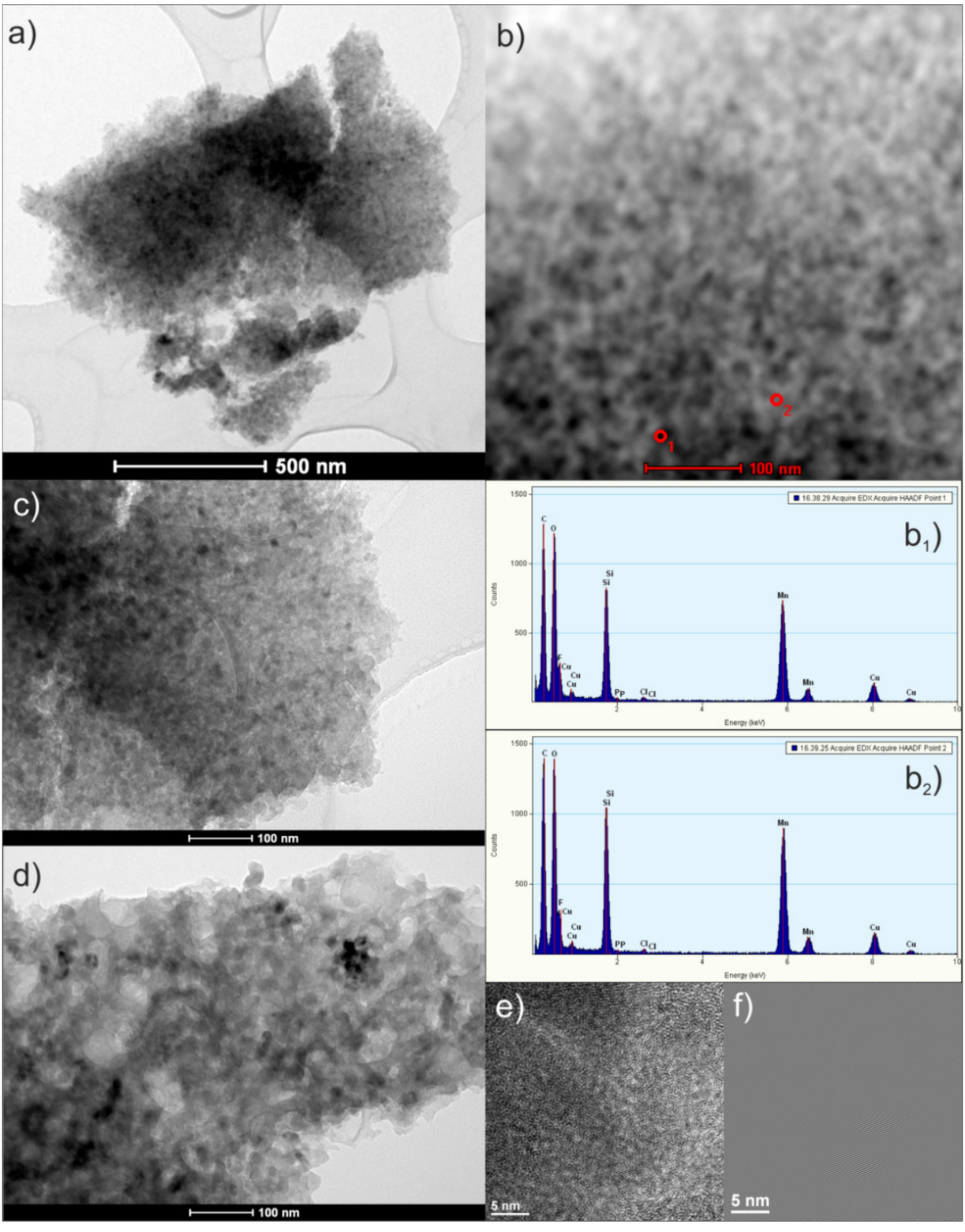

Figure 7. TEM micrographs of C/Li_2MnSiO_4@600. Micrographs a), c) and d) present bright field images of C/Li_2MnSiO_4@600 composite in different magnification; b) microstructure image observed in STEM-HAADF with EDS analysis (b_1; b_2) from marked points; e) high resolution micrograph (HREM) of a single grain and IFFT image f) from the same region.

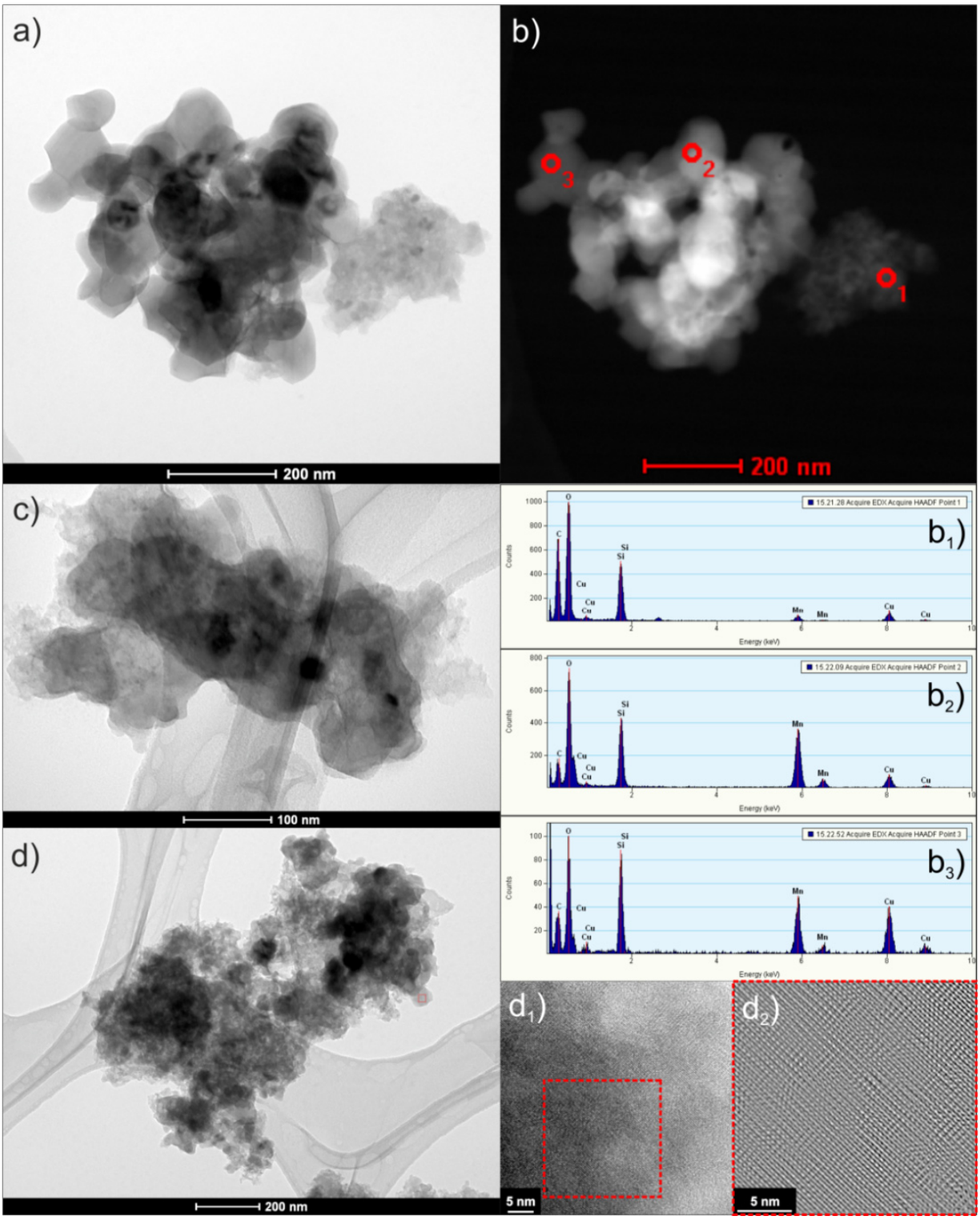

Figure 8. TEM micrographs of C/Li_2MnSiO_4@700. Micrographs a), c) and d) presents bright field images of C/Li_2MnSiO_4@700 composite in different magnification; b) microstructure image observed in STEM-HAADF with EDS analysis (b_1; b_2; b_3) from selected points; d_1) high resolution micrograph (HREM) of region marked in Fig. 8d; d_2) IFFT image from square marked in d_1).

STEM-HAADF image (Fig. 8b) from the same region as a bright field Fig. 8a shows points from where EDS analysis was conducted. All of lithium manganese orthosilicate crystallites in C/Li_2MnSiO_4@700 °C are well dispersed and fully covered in amorphous carbon. HREM image in Fig. 8d_1 with IFFT in Fig. 8d_2 shows crystalline structure of Li_2MnSiO_4 grain.

5. C/Li_2MnSiO_4 composite cathode material

Nevertheless obtained composites show homogeneous distribution of particles in carbon matrix and exhibit good electrical conductivity they work poorly in a battery cell (see paragraph 5.2). Thickness of primary carbon coating on active material grains strongly limits the electrochemical performance of composite.

5.1. CCL/Li_2MnSiO_4 composite preparation and properties

Preparation of composites with well define morphology of carbon layers and optimal carbon content was achieved by burning out the primary carbon and recoating Li_2MnSiO_4 nanosized grains with conductive carbon layers (CCL/Li_2MnSiO_4 composites). Burning out of primary carbon formed in the sample during synthesis process was carried through calcination of C/Li_2MnSiO_4@600 and C/Li_2MnSiO_4@700 under air flow at 300 °C for 3 h. CCL/Li_2MnSiO_4 composites were produced by wet polymer precursor deposition on active material grains and subsequent controlled pyrolysis [14, 20, 34]. Poly-N-vinylformamide (PNVF) obtained by radical-free polymerization of N-vinylformamide (Aldrich) with pyromellitic acid (PMA) additive (5-10 wt%) was used as a carbon polymer precursor [34]. To achieve an impregnation, Li_2MnSiO_4 grains were suspended in water polymer solution (8-15 wt%). Finally, samples were dried up in an air drier at 90 °C for 24 h. Prepared samples were pyrolyzed at 600 °C for 6 h under inert atmosphere (Ar).

Burning out primary carbon from the surface of lithium manganese silicate in air atmosphere leads to partial decomposition of active material. Fig. 9 shows XRD patterns of C/Li_2MnSiO_4@600, Li_2MnSiO_4@600 without carbon and CCL/Li_2MnSiO_4@600 composite after coating with CCL from polymer precursor.

In diffraction patterns of Li_2MnSiO_4@600 it is clearly visible that after burning out primary carbon layer new phase appears in the sample ($LiMn_2O_4$). Proposed carbon coating process can reverse decomposition of Li_2MnSiO_4. After coating Li_2MnSiO_4 (*Pmn2*$_1$) is a dominant phase in CCL/Li_2MnSiO_4@600 and all the lines, except for very low intensity line around 19°, can be associated with Li_2MnSiO_4 phase. CCL preparation procedure influence active material grain size. Average crystallite size calculated using Scherer equation in CCL/Li_2MnSiO_4@600 is ca. 25 nm. TEM analysis confirms increase of crystallites diameters. Li_2MnSiO_4 grains observed under TEM are in the range 25-75 nm. TEM micrographs of CCL/Li_2MnSiO_4@600 are presented in Fig. 10.

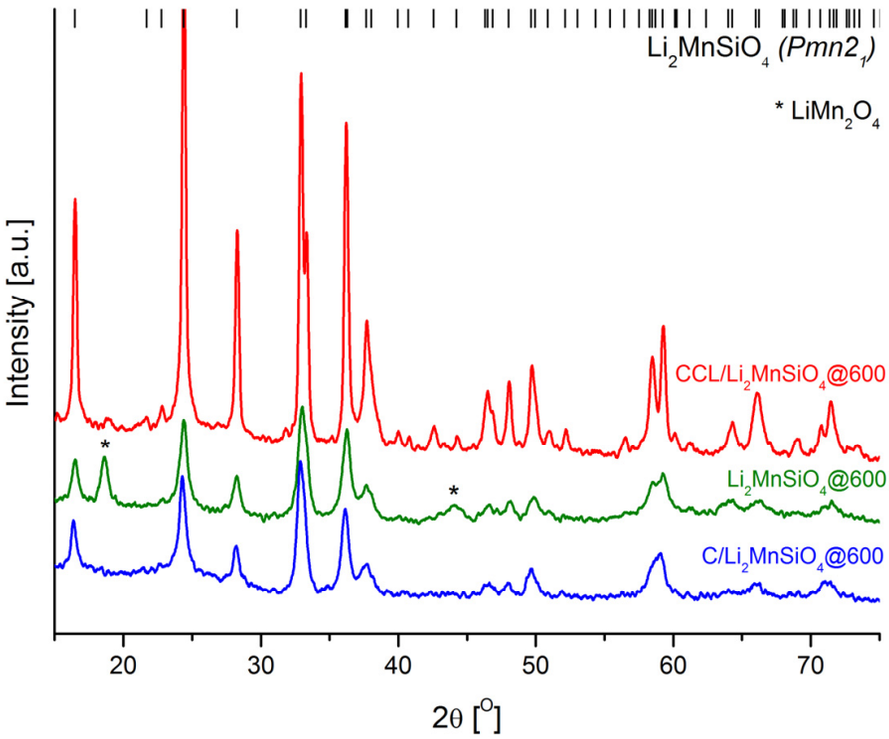

Figure 9. XRD patterns of C/Li_2MnSiO_4@600, Li_2MnSiO_4@600 and CCL/Li_2MnSiO_4@600.

Bright field micrographs (Fig. 10a, c, d) shows crystallites of Li_2MnSiO_4 covered with conductive carbon layers (CCL). Formed carbon coatings adhere well to the surface of active material grains, no voids are visible at the CCL/Li_2MnSiO_4 interface (Fig. 10e). Silicate grains are uniformly covered with approximately 4-5 nm thick CCL. EDS analysis once again confirm presence of lithium manganese silicate in the composite (Fig. 10b, b_1). Carbon content in samples was calculated from TPO measurements and they are displayed in Table 2.

Sample name	Precursor calcination temperature	Carbon content
CCL/Li_2MnSiO_4@600_7.5%	600 °C	7.5%
CCL/Li_2MnSiO_4@600_12%	600 °C	12%
CCL/Li_2MnSiO_4@700_5%	700 °C	5%
CCL/Li_2MnSiO_4@700_10%	700 °C	10%

Table 2. Carbon content of CCL/Li_2MnSiO_4 composites.

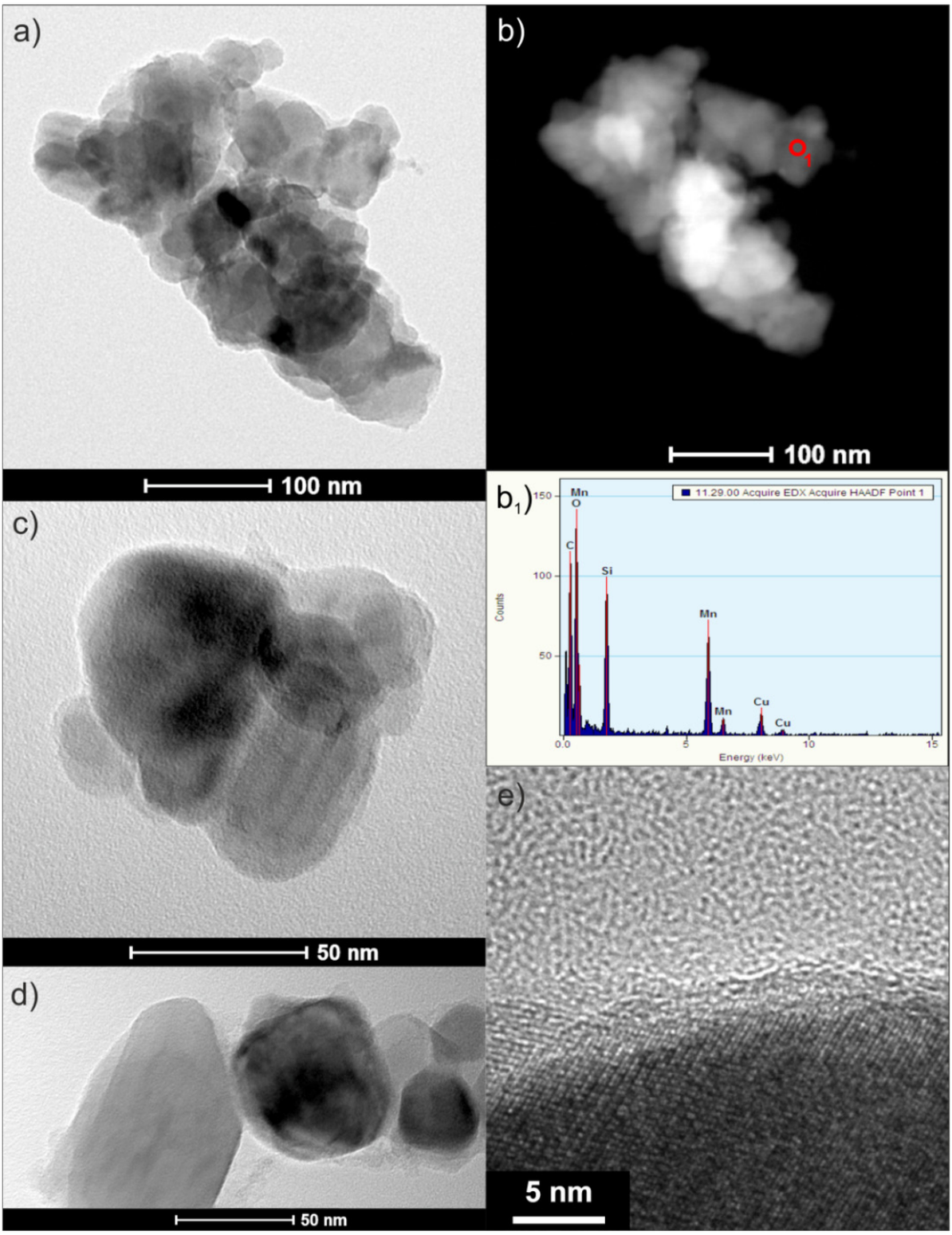

Figure 10. TEM micrographs of CCL/Li_2MnSiO_4@600. Micrographs a), c) and d) presents bright field images of CCL/Li_2MnSiO_4@600 composite; b) microstructure image observed in STEM-HAADF with EDS analysis (b_1) from selected point; e) HREM micrograph of carbon coating on the active material grain surface.

5.2. Electrochemical properties of C/Li_2MnSiO_4 composite cathode

The charge-discharge cycling studies of Li/Li^+/(C/Li_2MnSiO_4) cells were conducted in a four electrode configuration using CR2032 assembly between 2.7 and 4.7 V at C/200 rate at room temperature. $LiPF_6$ solution 1M in EC/DEC (1:1) was used in the cells as an electrolyte. The galvanostatic measurements were carried out using ATLAS 0961 MBI test system. Charge-discharge tests were conducted for all CCL composites listed in table 2, composites with primary carbon (C/Li_2MnSiO_4@600, C/Li_2MnSiO_4@700 and C/Li_2MnSiO_4@800) and standard composites (Li_2MnSiO_4@600_CB and Li_2MnSiO_4@700_CB). Standard composites were prepared by mixing Li_2MnSiO_4 powder with commercial carbon additive – carbon black (CB). 15 wt.% of carbon was used. Results collected from charge/discharge tests are presented in fig. 11-16.

C/Li_2MnSiO_4@600 sample did not show any reversible capacity (Fig. 11a). Lack of electrochemical activity of C/Li_2MnSiO_4@600 is connected with too high carbon loading. High carbon content (34%) is responsible for limiting of ionic conductivity in the composite and for surface polarization. Galvanostatic cycling studies of C/Li_2MnSiO_4@700 and C/Li_2MnSiO_4@800 revealed reversible capacity in a range of 30 $mAh \cdot g^{-1}$. Fig. 11b show charge and discharge capacity for 7 cycles of C/Li_2MnSiO_4@700 composite. After first four cycles reversible capacity stabilizes at about 30 $mAh \cdot g^{-1}$. Very poor performance of this sample is also connected with high amount of carbon in prepared composite (32%).

Standard composites obtained by mixing active silicate materials with carbon black (15%) show extremely low reversible capacity as well (Fig. 12a and 12b). In this case, carbon additive does not provide sufficient electrical contact between active material grains. Due to this fact, even under low C/200 rate samples performed very poorly in charge/discharge tests.

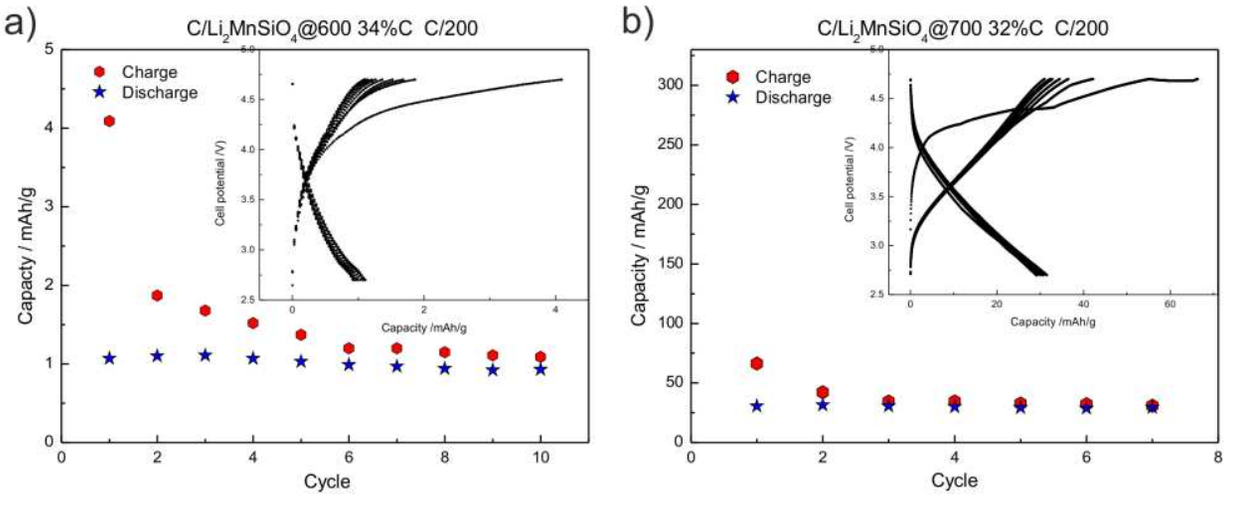

Figure 11. Cell cycling behavior of: a) C/Li_2MnSiO_4@600, b) C/Li_2MnSiO_4@700.

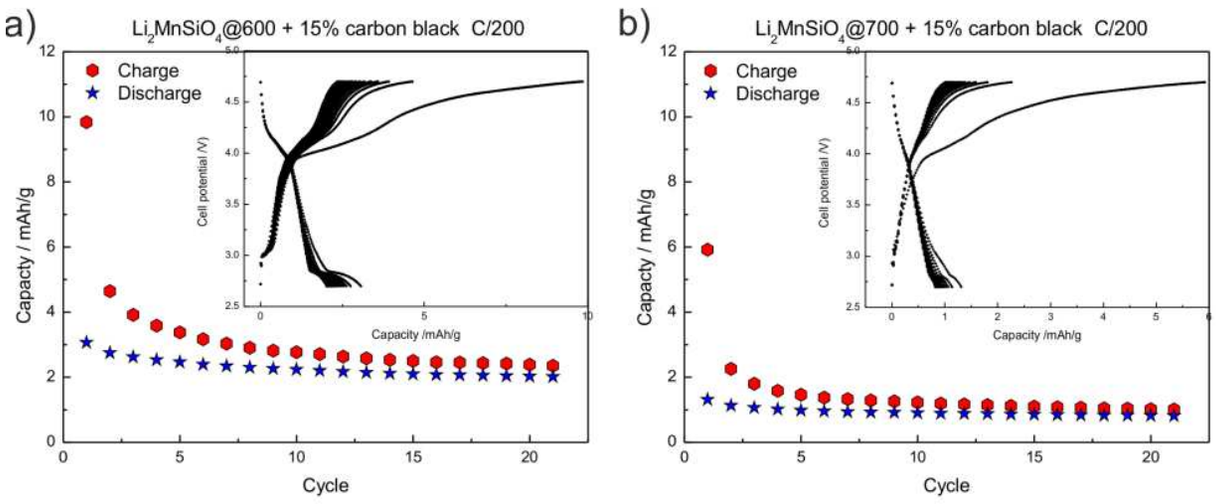

Figure 12. Cell cycling behavior of standard composites Li2MnSiO4 + carbon black (15% carbon content)

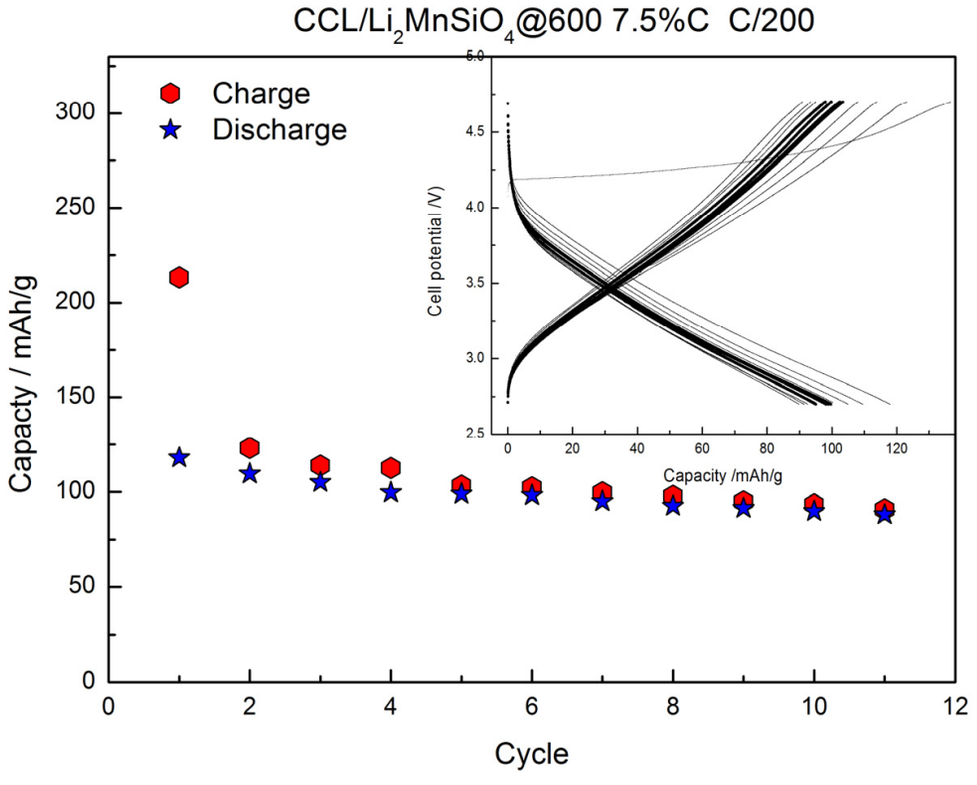

Figure 13. Cell cycling behavior of CCL/Li2MnSiO4@600 (7.5% carbon content)

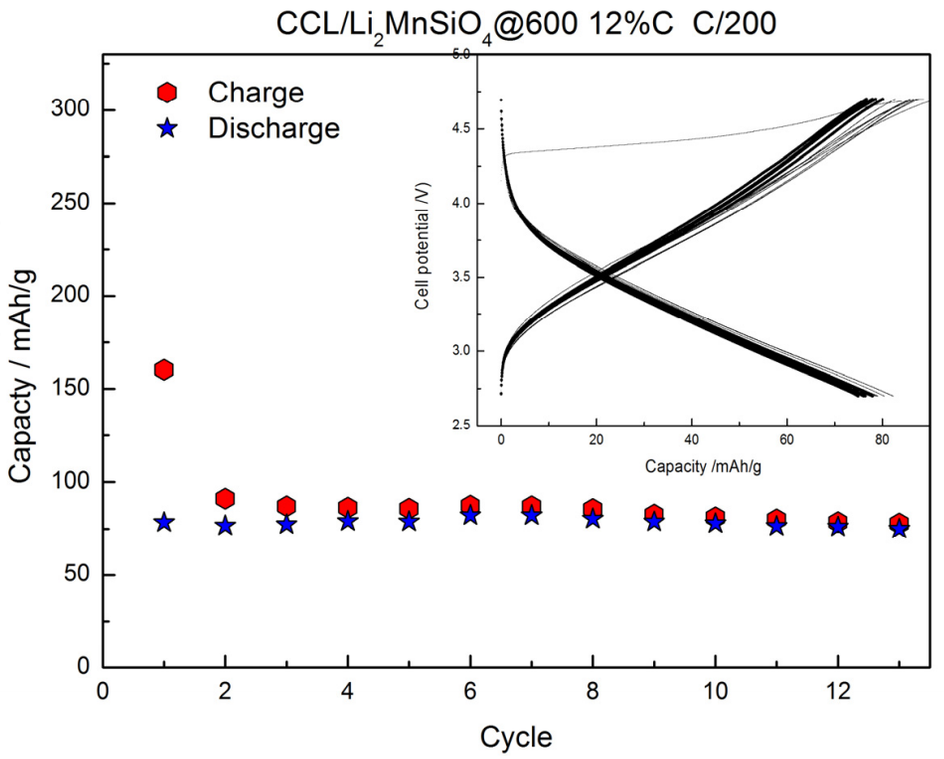

Figure 14. Cell cycling behavior of CCL/Li2MnSiO4@600 (12% carbon content)

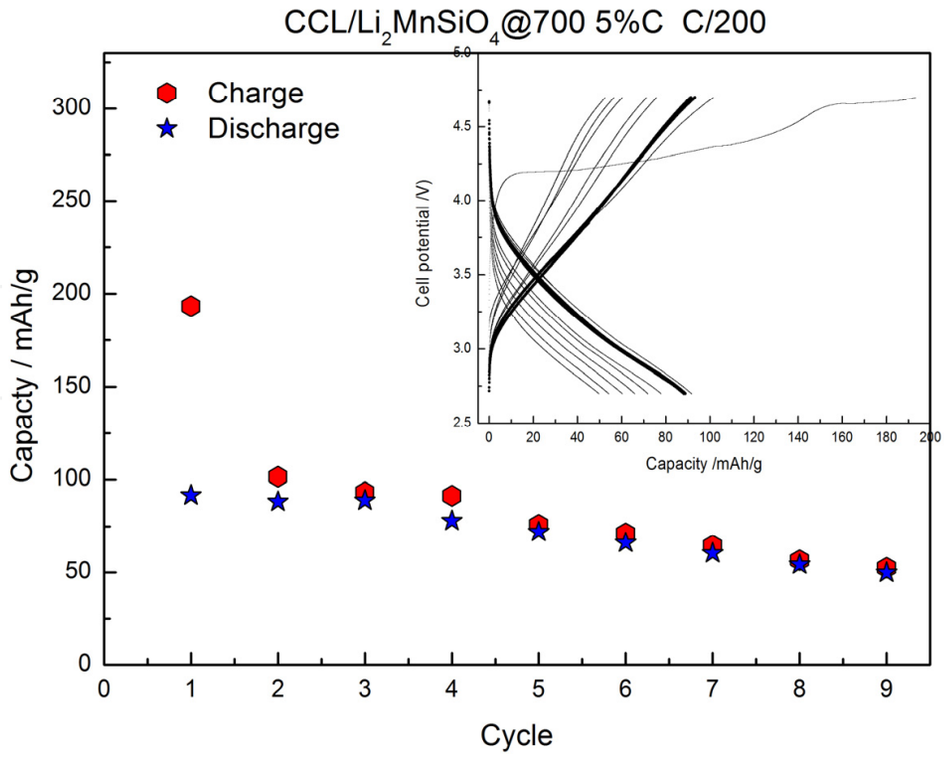

Figure 15. Cell cycling behavior of CCL/Li2MnSiO4@700 (5% carbon content)

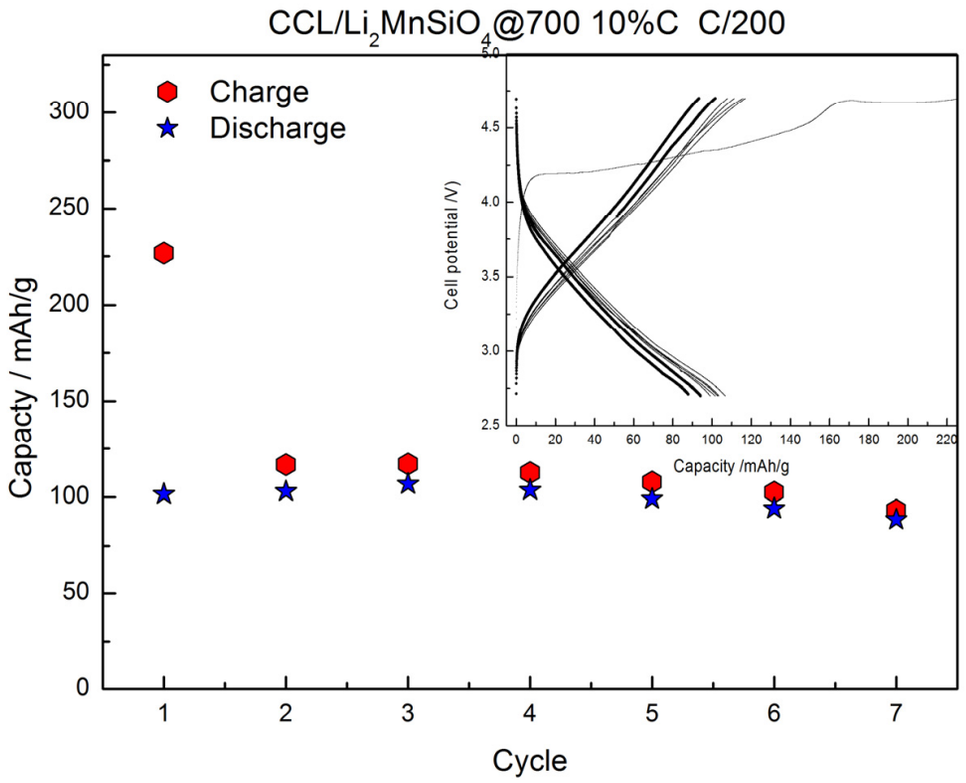

Figure 16. Cell cycling behavior of CCL/Li_2MnSiO_4@700 (10% carbon content)

Fig. 13-16 show cycling behavior of CCL composites with different amounts of carbon. Delithation of CCL composites after initial charging is in the range of 48-68% (charged CCL/Li_2MnSiO_4@600_12%C – correspond to composition $Li_{1.04}MnSiO_4$ and charged CCL/Li_2MnSiO_4@700_10%C – correspond to composition $Li_{0.64}MnSiO_4$). The observed capacity loss in the first cycles is related to SEI formation in CCL. During lithium extraction, Mn^{3+} and Mn^{4+} appear, and at the same time Li_2MnSiO_4 undergoes decomposition caused by Jahn-Teller distortion associated with changes in lattice parameters during $Mn^{3+} \rightarrow Mn^{4+}$ transition [30]. Despite the fact that crystalline structure collapses, discharge capacity is around 90-110 mAh/g. CCL composites produced from Li_2MnSiO_4 calcined at 600 °C exhibit better coulombic efficiency than Li_2MnSiO_4 calcined at 700 °C, the reversible capacity after 10 cycle is close to 100 mAh/g. The results indicate that coulombic efficiency of cathode material depends on grain size and homogeneity in grain size distribution, while cell capacity is limited by carbon coating performance.

6. Conclusions

Dilithium manganese orthosilicate – a high energy density cathode material – was successfully synthesized by sol-gel Pechini method. Encapsulation of nanosized grains of Li_2MnSiO_4 in carbon matrix, resulted from organic precursor, avoided further sintering. Different crystallite size was obtained, in particular, nanoparticles within range of 5-10 nm. High chemical stability of this material under a highly reductive environment was observed. Application of carbon coating improved electrical conductivity of cathode material to the

satisfactory level of ~$10^{-0.5}$ S/cm. Thickness of carbon coating on active material grains strongly limits the electrochemical performance of composite. Formation of CCL/Li_2MnSiO_4 composites significantly improved electrochemical performance of cathode materials, showing a reversible capacity of 90-110 mAh/g after 10 cycles. Electrochemical tests indicated that composite preparation should be optimized in terms of carbon content, CCL performance and homogeneity of a crystallite size. It was found that coulombic efficiency of cathode material depends on grain size and homogeneity in grain size distribution, while cell capacity is limited by carbon coating performance.

Author details

Marcin Molenda*, Michał Świętosławski and Roman Dziembaj
Jagiellonian University, Faculty of Chemistry, Krakow, Poland

Acknowledgement

This work has been financially supported by the Polish National Science Centre under research grant no. N N209 088638, and by the European Institute of Innovation and Technology under the KIC InnoEnergy NewMat project. The part of the measurements was carried out with the equipment purchased thanks to the financial support of the European Regional Development Fund in the framework of the Polish Innovation Economy Operational Program (POIG.02.01.00-12-023/08). One of the authors (M.Ś.) acknowledge a financial support from the International PhD-studies programme at the Faculty of Chemistry Jagiellonian University within the Foundation for Polish Science MPD. TEM analysis were carried out in Laboratory of Transmission Analytical Electron Microscopy at the Institute of Metallurgy and Material Science, Polish Academy of Sciences.

7. References

[1] Whittingham M.S. Electrical Energy Storage and Intercalation Chemistry. Science 1976;192 1126-1127.
[2] Nagaura T., Tozawa K. Lithium ion rechargeable battery. Progress in Batteries & Solar Cells 1990;9 209-217.
[3] Tarascon J.-M., Guyomard D. The $Li_{1+x}Mn_2O_4$/C rocking-chair system: a review Electrochimica Acta 1993;38(9), 1221-1231.
[4] Tarascon J.-M., Armand M. Issues and challenges facing rechargeable lithium batteries. Nature 2001;414(6861) 359-367.
[5] Zhang Z., Gong Z., Yang Y. Electrochemical Performance and Surface Properties of Bare and TiO_2-Coated Cathode Materials in Lithium-Ion Batteries. The Journal of Physical Chemistry B 2004;108(45) 17546–17552.

* Corresponding Author

[6] Molenda M., Dziembaj R., Podstawka E., Proniewicz L.M. Changes in local structure of lithium manganese spinels (Li:Mn=1:2) characterised by XRD, DSC, TGA, IR, and Raman spectroscopy. Journal of Physics and Chemistry of Solids 2005;66(10) 1761-1768.

[7] Dziembaj R., Molenda M. Stabilization of the spinel structure in $Li_{1+\delta/7}Mn_{2-\delta/7}O_4$ obtained by sol–gel method. Journal of Power Sources 2003;119–121C 121-124.

[8] Molenda J., Marzec J., Świerczek K., Ojczyk W., Ziemnicki M., Wilk P., Molenda M., Drozdek M., Dziembaj R. The effect of 3d substitutions in the manganese sublattice on the charge transport mechanism and electrochemical properties of manganese spinel. Solid State Ionics 2004;171(3-4) 215-227.

[9] Molenda M., Dziembaj R., Podstawka E., Proniewicz L.M., Piwowarska Z. An attempt to improve electrical conductivity of the pyrolysed carbon-$LiMn_2O_{4-y}S_y$ ($0 \le y \le 0.5$) composites. Journal of Power Sources 2007;174(2) 613-618.

[10] Molenda M., Dziembaj R., Podstawka E., Łasocha W., Proniewicz L.M. Influence of sulphur substitution on structural and electrical properties of lithium-manganese spinels. J. Phys. Chem. Solids 2006;67(5-6) 1348-1350.

[11] Chung K.Y., Yoon W.-S., Lee H.S., Yang X.-Q., McBreen J., Deng B.H., Wang X.Q., Yoshio M., Wang R., Gui J., Okada M. Comparative studies between oxygen-deficient $LiMn_2O_4$ and Al-doped $LiMn_2O_4$. Journal of Power Sources 2005;146(1-2) 226-231.

[12] Padhi A.K., Nanjundaswamy K.S., Goodenough J.B. Phospho-olivines as Positive-Electrode Materials for Rechargeable Lithium Batteries. Journal of the Electrochemical Society 1997;144(4) 1188-1194.

[13] Goodenough J.B., Kim Y. Challenges for Rechargeable Li Batteries. Chemistry of Materials 2010;22(3) 587-603.

[14] Molenda J., Molenda M. Composite Cathode Material for Li-Ion Batteries Based on $LiFePO_4$ System. In: Cuppoletti J. (ed.), Metal, Ceramic and Polymeric Composites for Various Uses. InTech; 2011.

[15] Padhi A.K., Nanjundaswamy K.S., Masquelier C., Okada S., Goodenough J.B. Effect of structure on the Fe^{3+}/Fe^{2+} redox couple in iron phosphates. Journal of the Electrochemical Society 1997;144(5) 1609-1613.

[16] Arroyo-de Dompablo M.E., Armand M., Tarascon J.M., Amator U. On-demand design of polyoxianionic cathode materials based on electronegativity correlations: An exploration of the Li_2MSiO_4 system (M = Fe, Mn, Co, Ni). Electrochemistry Communication 2006;8 1292-1298.

[17] Gong Z.L., Li Y.X., Yang Y. Synthesis and electrochemical performance of Li_2CoSiO_4 as cathode material for lithium ion batteries. Journal of Power Sources 2007;174(2) 524-527.

[18] Nyten A., Abouimrane A., Armand M., Gustafsson T., Thomas J.O. Electrochemical performance of Li_2FeSiO_4 as a new Li-battery cathode material. Electrochemistry Communication 2005;7(2) 156-160.

[19] Kokalj A., Dominko R., Mali G., Meden A., Gaberscek M., Jamnik J. Beyond One-Electron Reaction in Li Cathode Materials: Designing $Li_2Mn_xFe_{1-x}SiO_4$. Chemistry of Materials 2007;19(15) 3633-3640.

[20] Molenda M., Dziembaj R., Drozdek M., Podstawka E., Proniewicz L.M. Direct preparation of conductive carbon layer (CCL) on alumina as a model system for direct

preparation of carbon coated particles of the composite Li-ion electrodes. Solid State Ionics 2008; 179(1-6) 197-201.

[21] Sirisopanaporn C., Boulineau A., Hanzel D., Dominko R., Budic B., Armstrong A.R., Bruce P.G., Masquelier C. Crystal Structure of a New Polymorph of Li_2FeSiO_4. Inorganic Chemistry 2010;49(16) 7446-7451.

[22] Boulineau A., Sirisopanaporn C., Dominko R., Armstrong A.R., Bruce P.G., Masquelier C. Polymorphism and structural defects in Li_2FeSiO_4. Dalton Transactions 2010;39(27) 6310-6316.

[23] Sirisopanaporn C., Masquelier C., Bruce P.G., Armstrong A.R., Dominko R. Dependence of Li_2FeSiO_4 Electrochemistry on Structure. Journal of the American Chemical Society 2011;133(5) 1263-1265.

[24] Mali G., Rangusa M., Sirisopanaporn C., Dominko R. Understending ^6Li MAS NMR spectra of Li_2MSiO_4 materials (M=Mn, Fe, Zn). Solid State Nuclear Magnetic Resonance 2012;42 33–41.

[25] Liu W., Xu Y., Yang R. Synthesis, characterization and electrochemical performance of Li_2MnSiO_4/C cathode material by solid-state reaction. Journal of Alloys and Compounds 2009;480(2) L1-L4.

[26] Karthikeyan K., Aravindan V., Lee S.B., Jang I.C., Lim H.H., Park G.J., Yoshio M., Lee Y.S. Electrochemical performance of carbon-coated lithium manganese silicate for asymmetric hybrid supercapacitors. Journal of Power Sources 2010;195(11) 3761-3764.

[27] Gummow R.J., Sharma N., Peterson V.K., He Y. Crystal chemistry of the *Pmnb* polymorph of Li_2MnSiO_4. Journal of Solid State Chemistry 2012;188 32-37.

[28] Gummow R.J., Sharma N., Peterson V.K., He Y. Synthesis, structure, and electrochemical performance of magnesium-substituted lithium manganese orthosilicate cathode materials for lithium-ion batteries. Journal of Power Sources 2012;197 231-237.

[29] Molenda M., Swietoslawski M., Rafalska-Lasocha A., Dziembaj R. Synthesis and Properties of Li_2MnSiO_4 Composite Cathode Material for Safe Li-ion Batteries. Functional Material Letters 2011;4(2) 135-138.

[30] Dominko R., Bele M., Kokalj A., Gaberscek M., Jamnik J. Li_2MnSiO_4 as a potential Li-battery cathode material. Journal of Power Sources 2007;174(2) 457-461.

[31] Li Y.X., Gong Z.L., Yang Y. Synthesis and characterization of Li_2MnSiO_4/C nanocomposite cathode material for lithium ion batteries. Journal of Power Sources 2007;174(2) 528–532.

[32] Aravindan V., Ravi S., Kim W.S., Lee S.Y.,. Lee Y.S. Size controlled synthesis of Li_2MnSiO_4 nanoparticles: effect of calcination temperature and carbon content for high performance lithium batteries. Journal of Colloid and Interface Science 2011;355(2) 472–477.

[33] Swietoslawski M., Molenda M., Zaitz M., Dziembaj R. C/Li_2MnSiO_4 as a Composite Cathode Material for Li-ion Batteries, ECS Transaction 2012;41 – *in press*

[34] Molenda M., Dziembaj R., Kochanowski A., Bortel E., Drozdek M., Piwowarska Z. Process for the preparation of conductive carbon layers on powdered supports Int. Patent Appl. No. WO 2010/021557, US Patent Application 20110151112.